Sensors for anaerobic hydrogen measurement: A comparative study between a resistive PdAu based sensor and a commercial thermal conductivity sensor

Clément Occelli, Tomas Fiorido, Carine Perrin-Pellegrino, Jean-Luc Seguin

Sensors for anaerobic hydrogen measurement: a comparative study between a resistive PdAu based sensor and a commercial thermal conductivity sensor.

Clément Occelli, Tomas Fiorido, Carine Perrin-Pellegrino, Jean-Luc Seguin

Aix-Marseille Univ, Univ Toulon, CNRS, IM2NP

Marseille, 13397, France

e-mails : {clement.occelli, tomas.fiorido, carine.perrin-pellegrino and jean-luc.seguin}@im2np.fr

Corresponding author: clement.occelli@im2np.fr

Abstract : Hydrogen sensors able to perform measurements in real time in anaerobic environment such as natural gas (NG) will greatly help the development of power to gas technology. For now, thermal conductivity (TC) gas sensors and Pd thin film based sensors have demonstrated their capability to measure H_2 in air and N_2 but there is still lack of testing in natural gas environment. In this study, the sensing performances (response, hysteresis, response time and selectivity) of two sensors were assessed in three anaerobic environments: N_2, CH_4, and NG. The first one is a homemade resistive sensor based on a PdAu thin film and the second one is a commercial thermal conductivity sensor. While most performances are equivalent for both technologies, only the PdAu sensor is able to detect selectively H_2, without any interfering effect with NG components. Thus, Pd based thin film sensors are promising for H_2 detection in anaerobic environments.

Keywords : Hydrogen sensors; Resistive sensor ; Thermal conductivity sensor; Power-to-gas; Anaerobic; Palladium gold (PdAu)

1. Introduction

The current context of climate change and the drive for sustainable development require the reduction of greenhouse gas emissions through the introduction of new technologies with minimal or no carbon emissions. Hydrogen gas has been identified as a very attractive energy carrier, since its combustion and its use to produce electricity generate only water as by-products [1], [2]. However, hydrogen in its molecular form H_2 cannot be found in exploitable quantities in nature and so has to be produced. Nowadays, hydrogen production arises at 96% from fossil fuel sources (grey hydrogen) such as natural gas (49%), liquid hydrocarbon (29%) and coal (18%); only 4% of hydrogen is produced from water splitting techniques such as electrolysis [3].

A possible alternative for reduction of greenhouse gas emission is the replacement of current carbon intensive hydrogen production by water electrolysis using only electricity from renewable energy sources, also known as green hydrogen [4]. For the moment, green hydrogen prices are not as competitive as grey ones, with prices per kilo being at least three time higher. A promising technology to reduce transportation costs, energy conversion losses and increase storage time, is the injection of green hydrogen in gas pipelines, also known as Power to Gas (P2G) [3].

The purpose of P2G is to produce green hydrogen from water electrolysis, using only the surplus of electricity production from renewable energy sources [5]. This hydrogen is then either directly injected in natural gas (NG) grid or used to produce CH_4 with captured CO_2 following the Sabatier reaction. A schematic representation of P2G principle is shown in Fig. 1. The use of gas pipelines to transport hydrogen (as a H_2/NG mixture) toward the end user allows to avoid construction of new costly infrastructures and facilitates long term storage [6]–[8]. In addition, P2G has other advantages such as seasonal storage as well as reduced emissions and consumption, when using a 10% H_2/NG mix [9]–[12].

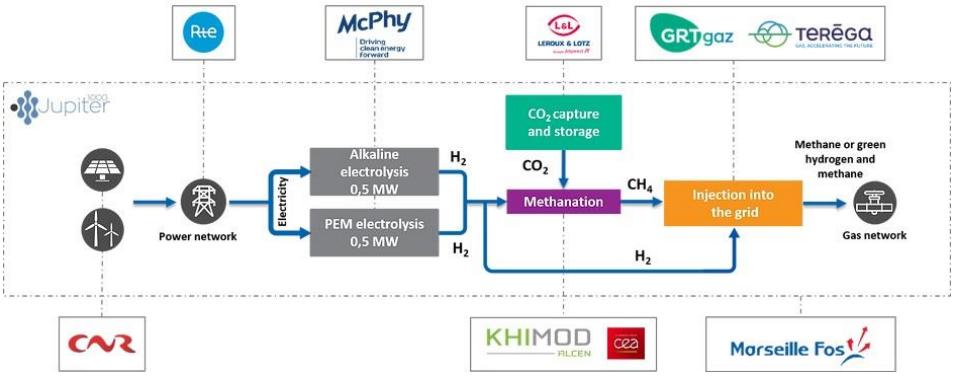

Fig. 1. Power to gas principle for French demonstrator : Jupiter 1000 [13].

However, Power to gas technology will face several constraints:

- Maximal concentration level: hydrogen being the lightest of chemical elements and the smallest molecule, it has a great propensity to leak and to permeate through many materials causing embrittlement. Recent studies show that low hydrogen partial pressure (ca. 100 to 200 kPa) has little to no effect on pipeline materials such as austenitic, ferritic or stainless steel and even elastomer/polymer ones, as long as it is defect free [14], [15]. Reports tend to conclude that current gas grid may not be suited for high H_2 concentrations without considerable upgrade. For now, H_2 concentration is not considered to be higher than 6 to 10% [5], [16]. In the light of these results, particular attention should be paid to the respect of maximal injection value to not shorten pipelines life time.
- Gas quality variation: commercial natural gas is a mixture of various hydrocarbons, with methane accounting for 70 to almost 100%, and inert diluents such as N_2 and CO_2. Renewable energy being intermittent by nature, the production and thus injection of H_2 will also fluctuate, leading to gas quality variability. This is of major concern as gas engines and turbines optimal operating parameters are dependent on the gas quality. Any fluctuation in composition will affect thermodynamic properties of combustion (specific heat, flame temperature) [17] and so engine performances, gas emissions (NOx, CO, CO_2), fuel consumption and durability [10], [17], [18].

Common technology used in industry to control hydrogen level is based on gas chromatography [19], which is expensive and do not allow real time information (sampling analyse), or on complex modelling that may lack of accuracy [20]. Hence, the development of P2G will imply hydrogen sensors, able to detect in real time, at many points of the supply chain, wherever hydrogen is produced, transported and used.

Nowadays, most of commercially available hydrogen sensors are mainly based on three technologies : catalytic, conductometric based on semi conductive metal oxides (SMOx) and electrochemical [21], [22]. However, these sensors are developed to detect hydrogen leaks and thus are designed to operate in air, under oxygen. In gas pipelines, impurities such as humidity, O_2 and SO_2 are kept to a minimum to limit corrosion and embrittlement [23]. As a result, output gas can be considered as an almost perfectly dry and completely anaerobic environment. The technologies presented above need either oxygen environment to operate [24] or humid conditions [25], [26] and will not be suitable to measure hydrogen concentrations in H_2/NG mixtures. While sensors for the detection of hydrogen leaks into the air have been widely studied for decades [27]–[29], only few studies focus on the measurement of high hydrogen concentrations in an oxygen-deprived atmosphere.

According to Buttner work [30], promising technologies to detect H_2 under oxygen deprived atmosphere are either thermal conductivity sensor (TC) or palladium thin film (PTF) sensor. The first one measures the heat losses from a hot body exposed to environment. While the second one measures the variation of the physical properties of the thin film (conductivity, optical index) due to the reaction of H_2 with palladium, leading to hydride formation. However, the sensors were only studied in H_2/Air or H_2/N_2 mixtures. Similarly, other work also demonstrate the ability of PdAu thin film to detect H_2 in anaerobic condition but for hydrocarbon binary gas mixture [31]. PdAu alloy is known to be more advantageous than pure Pd, as it is hysteresis-free and exhibits a faster hydrogen absorption [32], [33]. In our previous work [34], we presented preliminary result on PdAu (20%) based resistive sensor made by co-sputtering. Sensor was found to be suited for hydrogen measurement in anaerobic conditions from 0 to 3% (maximal test condition). The goal of present paper is to assess and compare the performances of two technologies, a commercial thermal conductivity (TC) gas sensor with our simply designed and fabricated PdAu resistive sensor, for the specific application to P2G. The response, hysteresis, response time and selectivity to hydrogen of both sensors in anaerobic atmospheres containing either N_2, CH_4, or synthetic natural gas are presented. The results show that PdAu based resistive sensor perfectly meets the requirements for hydrogen measurements in NG : they can measure up to 3% hydrogen without hysteresis and without any cross sensitivity with NG components.

2. Tested sensors presentation

2.1. PdAu based resistive sensor

2.1.1. Detection principle

The detection principle of PTF sensor lays on the reversible absorption and desorption of H_2 from Pd bulk. Absorbed H atoms occupy octahedral interstitial sites from the fcc structure, resulting in physical properties modifications such as electrons scattering that induce a drop in the material conductivity. The absorption of Pd follows approximately the Sievert's law [35] meaning that the amount of absorbed H atoms depends on the square root of the H_2 partial pressure. Following previous statements, a specific increase in H_2 partial pressure will result in a specific increase in film resistance [36]. Thus, it is easily possible to follow H_2 concentration fluctuations and measure accurate values.

However, the use of pure Pd as a sensitive film is quite limiting. Indeed, pure Pd thin films exhibit quite long response and recovery times and a quite stable hydride. Also, thin films exhibit an important hysteresis [37] and degrade under repeated exposures due to the α to β phase transition [38].

One solution to avoid these serious drawbacks is to introduce, into Pd, metal atoms with an atomic radius larger than that of Pd atoms, e.g. gold (Au) atoms. Hence, Au atoms, which occupy Pd lattice sites, slightly expand it, which modifies the thermodynamic properties of hydrogen solution in Pd [39]. As a result, hysteresis shrinks, phase transition disappears, and response and recovery times drop, but at a price of a slight sensitivity decrease [39]–[41]. According to literature, the best compromise is found around 20-25% Au content. The following parts will present the fabrication and characterization of said sensor for optimal composition.

2.1.2. Sensor fabrication

PdAu deposition was made by radio frequency magnetron sputtering, see Fig. 2.a) and 2.c), according to the process described in [34]. Two cleaned substrates were placed in the sputtering chamber: one for structural characterization (sample A), the other for sensor realization (sample B). To allow rapid characterization of hydrogen sensing, a simple basic sensor was made using a shadow mask consisting of a thin sheet of steel mechanically drilled. A picture of the fabricated sensor with his mask is shown in Fig. 2.b). Once deposition completed, the samples were annealed at 200°C in N_2 gas for several hours, since 200°C was found to be the best annealing temperature to promote hydrogen absorption sites [42]. Finally, a 120nm thick film was obtained.

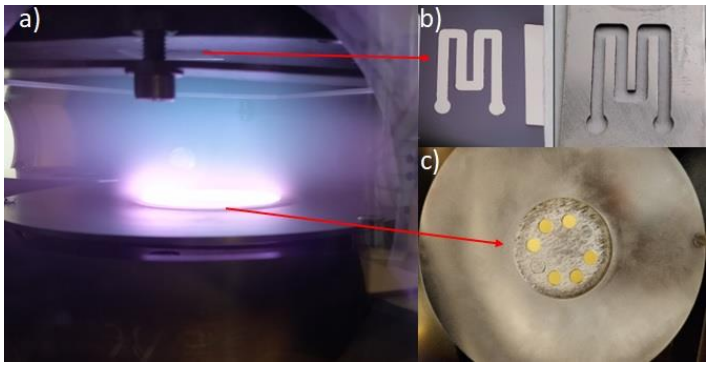

Fig. 2. PdAu sensor fabrication, a) Sputtering device, b) Mechanical mask and as-deposited sensor, c) Pd sputtering target with gold disks.

2.1.3. Chemical composition

Scanning Electron Microscopy (SEM) analysis was performed with a Zeiss Gemini SEM 500. The SEM picture presented in our previous paper [34] show a dense structure composed of zones with small grains (around 20nm) and zones of merged grains. For chemical analysis, an Energy Dispersive X-rays Spectroscopy (EDS) was done at 15 kV, with a magnification of 10k on 3µm x 3µm area. Fig. 3 shows X-ray line spectra performed on sample A, with detected elements such as Palladium (Pd), Gold (Au), and Silicon (Si). Four measurements were performed revealing an estimated alloy composition of 80% Pd and 20% Au.

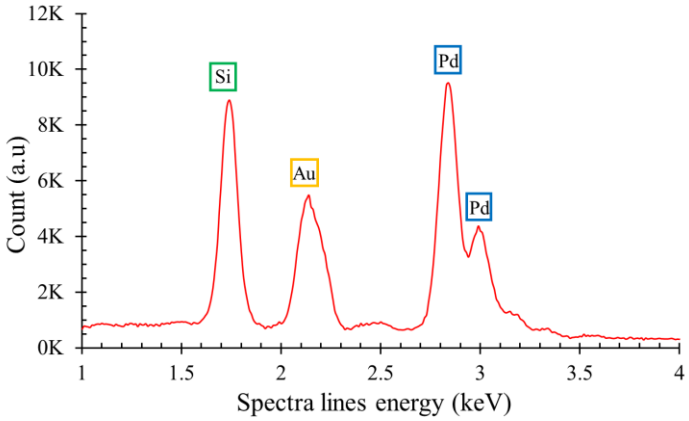

Fig. 3. EDS performed on sample A; for ease of reading, Au peak at 9.72 keV is not displayed.

2.1.4. X-ray diffraction

The sample A microstructure was examined by X-ray diffraction (XRD), prior and after annealing. Fig. 4 evidences that, for our sputtering parameters and film thickness, the film crystallizes mainly with a (111) preferred orientation and this trend is kept even after annealing. Small diffraction peaks are detected for the (311) and (222) planes. Heat treatment has a noticeable impact on the microstructure with an increase of the crystallinity as (111) peak intensity grows from 13700 to almost 19400 counts. The grain size estimated from the Scherrer formula seems to be stable around 20 ±1 nm. Otherwise, the 2θ angle shift of the diffraction peaks is suggesting stress relaxation during the heat treatment.

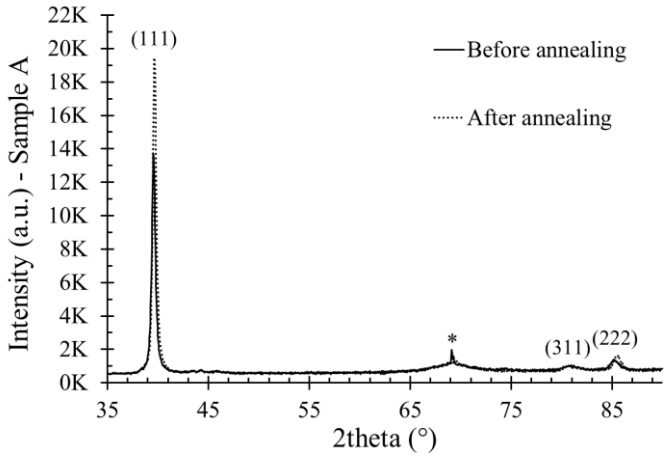

Fig. 4. XRD diagram of sample A before and after annealing (λ=0.154 nm). The star indicates the trace of the Si substrate diffraction peak.

2.1.5. Preliminary testing for sensors comparison

In our previous work, we determined that 323 K was the best operating temperature, as it combines not excessively long response and recovery times, a satisfactory response amplitude and a clear signal [34]. In the following work, all tests will be performed at a temperature of 323 K.

In order to efficiently evaluate the performances of both sensors, the analytics signals have to be comparable. Thus the resistive sensor output was converted to a hydrogen concentration value based on a series of hydrogen step measurements ranging from 0 to 3% H_2, with start exposures at 0.1%, 0.2%, 0.3% and then step increase of 0.3% H_2. Sensor response, $R_S(\%)$, is calculated based on formula 1, where r_0 is the value of sensor stable base line resistance under constant temperature and carrier gas flow (value taken once, before any H_2 exposure), and r is the value of the sensor electrical resistance under H_2 exposure.

$$R_S(\%) = [(r-r_0)/r_0]\times 100 \qquad (1)$$

To determine the relationship between sensor resistance and hydrogen concentration, we can use the empirical relation known as the Sievert's law, assuming that the atomic concentration of hydrogen in a solid metal [H] is proportional to the square root of the hydrogen partial pressure [H_2], Since the response of the sensor, $R_S(\%)$, is proportional to the atomic concentration of hydrogen in the metal, we can write equation 2, K being a constant. Inverting this relationship, we find equation 3. By fitting the data to a quadratic law, at a given temperature, it is

possible to obtain the hydrogen concentration (referred below as $C_R(\%)$) as a function of the sensor resistance [35]. However, when using a 2nd-order polynomial, some data points are not on the fitted curve. We obtained a better accuracy with a 5th-order polynomial, although it has no physical meaning. Fig. 5 shows the plot of hydrogen concentration as a function of sensor response and the determined polynomial equation.

$$R_S = K[H_2]^{1/2} \quad (2)$$

$$[H_2] = (R_S/K)^2 \quad (3)$$

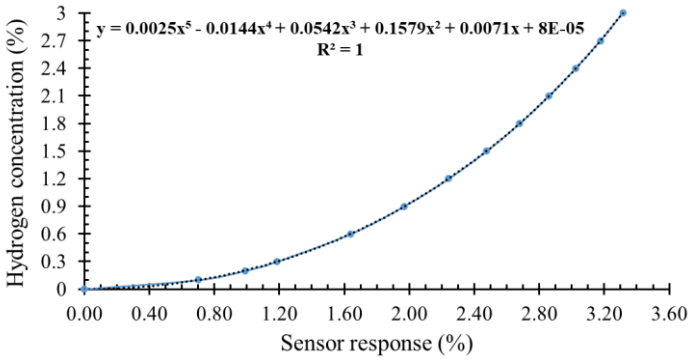

Fig. 5. Best fit of data points using a 5th order polynomial for sensor response conversion to concentration response.

2.2. Thermal conductivity sensor

2.2.1. Detection principle

The principle of thermal conductivity (TC) gas sensors is based on the measurement of the heat loss from a hot body to the surrounding atmosphere. Common TC sensors are made using MEMs (micro-electro-mechanical system) technology [43] although recent work shows that the use of metallic wire based on current sweep to be effective for detection as well [44]. A thin resistor film protected by an inert coating in order to prevent any chemical reaction is placed on a suspended membrane etched on a silicon chip. The resistor film acts for both heating the membrane and detecting its temperature. Depending on the thermal conductivity of the gas flowing around the membrane, more or less energy is taken from the membrane. The electrical power needed to maintain the membrane's temperature constant is a direct measure of the thermal conductivity [29], [30].

2.2.2. Commercial Blue Vary technical specification

In the case of our commercial TC sensor, two resistors films are integrated into the membrane. Furthermore, in order to prevent from ambient temperature influence, the micromechanical chip is fitted into a housing that operate at a constant temperature of 60°C. The whole housing is then placed in a cartridge that can easily be plugged on a pipe. The cartridge is operated by the commercial station. Data measurements are recovered by connecting the device to a PC USB port. Only 1 point per 10 seconds can be recorded. Prior to sensor measurement, a 1 point calibration is required. Due to sensor drift in time (0.2% of value per month) the calibration is performed at least once a month. The standard procedure consists to expose the sensor to a continuous N_2 flow of 200 sccm or higher for at least 30 min. The calibration procedure is effective when output value for H_2 measurement is almost null (< 0.01%). Device operate on 0-10% measuring range. The accuracy is about ± 5% of measured value ± 0.5% of range [45]. The sensor is suited for operation around atmospheric pressure (80 – 130 kPa absolute), at ambient temperature (278 – 328 K) from low to high relative humidity (0-100% RH) [45]. It is then perfectly suited for our experimental conditions.

3. Experimental setup and test configurations

3.1. Bench configuration

Both sensors were tested, using the same experimental setup. A schematic representation of our test bench is displayed in Fig. 6. The experimental facilities are composed of:

- An ATEX (Atmospheres Explosibles) gas enclosure, where all combustible gas bottles are stored and plugged to a steel pipe that carry the gas to the bench. Five gas bottles are available and changed depending on test needed, bottles concentrations are given in table 1.
- A programmable gas dilution system using mass flow controllers. Maximal flow is 400 sccm for 2 bottles configuration and 200 sccm for 3 bottles configuration.

- The resistive PdAu tested sensor is placed in a cross shaped test chamber as displayed in Fig. 6 (named "cross chamber" in the following), of approximately 400 cm^3. The sensor is positioned on a heating plate with a Pt100 (class B accuracy) temperature sensor attached next to it for thermal regulation. The electrical resistance of the sensing film is measured by a Keithley 2450 Sourcemeter and recorded on a personal computer by a homemade software, every 0.5s. The commercial TC sensor operates autonomously and is simply connected to an USB port to collect data.

Two test configurations will be used:

- In configuration 1 : either the resistive sensor or the commercial TC sensor is connected to the dilution system and exposed to the carrier gas.
- In configuration 2 : the commercial TC sensor is placed right after the cross chamber. This configuration will be used to assess the influence of the important volume of the cross chamber on response time, or to compare sensors selectivity.

3.2. Exposure profiles and characterization parameters

Tests are performed using either pure N_2 or synthetic natural gas as a baseline from bottles. Prior to test, sensors are flushed at the test flow, a few hours, with the carrier gas, to ensure dry and anaerobic conditions. Also, the resistive PdAu sensor is heated to 223 K and let to stabilize before any exposure. Similar operation is performed on TC sensor, as a 60 min heating is required in order to operate. Each following hydrogen exposure last 25 min.

Step exposure: this test consists of a gradual hydrogen concentration increase by steps of 0.1% from 0 to 0.3% and then by steps of 0.3% from 0.3 to 3%. Once 3% is reached, the concentration decreases to 0% following the reverse process.

Pulse exposure: the sensors are exposed to a single hydrogen concentration and then flushed with carrier gas for 2 hours, operation is repeated for a higher concentration value. Exposition ranges from 0.3 to 3% with 0.3% increase.

Exposure to interfering gas: series of 3 pulses at 0.9% H_2 are performed in various content of interfering gases. Before and after each hydrogen pulse, sensors are flushed by the carrier gas that may contain interfering gas. This series of tests begins in pure N_2 atmosphere for reference. After 3 pulses, interfering gas content or nature changes.

Once PdAu resistive sensor calibrated, the signals of both sensors can be compared. Only concentration response, $C_R(\%)$, will be discussed below. For each H_2 concentration, the corresponding sensor $C_R(\%)$ is measured by averaging data on the last 1 min exposure.

Hysteresis is determined by exposing sensors to continuous flow of hydrogen in N_2 following the step exposure profile described earlier. $C_R(\%)$ is determined for both ascending and descending phase. Hysteresis is the difference in $C_R(\%)$ value between the descending and rising phase. For a given hydrogen concentration, a positive hysteresis implies a higher $C_R(\%)$ on descending phase compared to ascending one and vice versa.

The response and recovery times, presented below, are respectively defined as the time needed to reach 90% of the maximal $C_R(\%)$ value for a given H_2 exposure (T_{90}) and as the time needed to return from stable $C_R(\%)$ value to 10% of the stable baseline when hydrogen gas was stopped (T_{10}).

Sensor selectivity was evaluated by measuring the sensor baseline and sensor concentration response to 0.9% H_2 in the presence and absence of interfering species (CH_4, synthetic NG). Two cross sensitivity factors will be used: $X^i_0(\%)$ and $X^i_H(\%)$

- $X^i_0(\%)$ is the baseline variation after interfering gas was injected, see eq (4); C_i is the concentration response to the interfering specie and C_0 the baseline value in N_2.
- $X^i_H(\%)$ is the ratio of sensor response to 0.9% hydrogen in interfering gas on sensor response to 0.9% H_2 in N_2 gas, see eq(5), C_H and $C_{H,i}$ being respectively the concentration response to hydrogen in N_2 and the concentration response to hydrogen in the interfering atmosphere.

In other word, $X^i_0(\%)$ is the sensor concentration response to interfering gas, while $X^i_H(\%)$ represents the percentage variation of sensor $C_R(\%)$ to 0.9% H_2 in presence of interfering gas. The contaminant has no influence on sensor response when the value for $X^i_0(\%)$ and $X^i_H(\%)$ are both equal to zero. Values are averaged on 1 min of data, C_i and C_0 are averaged once, after 30 min carrier gas flush, C_H and $C_{H,i}$ are averaged on the last minute of three hydrogen pulses.

$$X^i_0(\%) = C_i - C_0 \qquad (4)$$

$$X^i_H(\%) = ([(C_{H,i} - C_i)/(C_H - C_0)] - 1) \times 100 \qquad (5)$$

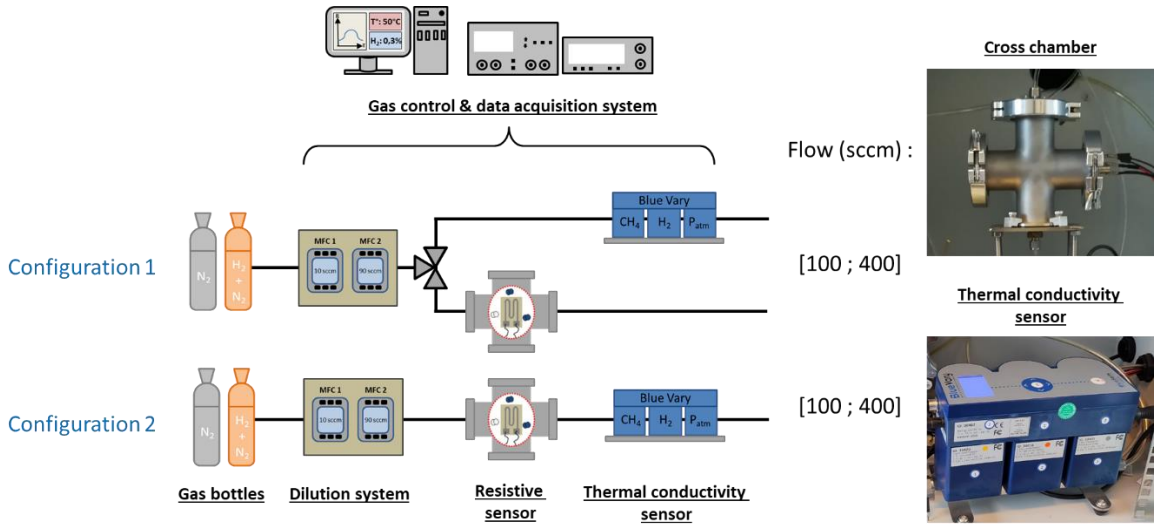

Fig. 6. Experimental setup and test configuration.

Gas bottle	Composition
Nitrogen (Baseline 1)	Pure N_2
Methane	Pure CH_4
Synthetic Natural Gas (Baseline 2)	72.07% CH_4 ; 14.04% N_2; 8.97% CO_2 ; 2.98% C_2H_6 ; 0.96% C_3H_8 ; 0.98% C_4H_{10}
Hydrogen in Nitrogen	97% N_2 ; 3% H_2
Hydrogen in Synthetic Natural Gas	72.06% CH_4 ; 12.03% N_2; 7.97% CO_2 ; 3.01% H_2; 2.98% C_2H_6 ; 0.96% C_3H_8 ; 0.98% C_4H_{10}

Table 1. Gas bottle composition (the accuracy of gas mixture is better than 10% and their stability guaranteed for 36 months).

4. Experimental results and discussion

4.1. Response to hydrogen exposures

Sensors were exposed to a series of different hydrogen concentrations following pulse and step exposure profile. Both tests were performed in configuration 1 at a flow rate of 100 sccm. The tests results are presented on Fig. 7 and matched with corresponding set point recipe (grey curve). Fig. 7.a &b show that both sensors are sensitive to hydrogen concentration either by pulse or step exposure respectively, ranging from 0.1 or 0.3 to 3%. A full recover and a stable baseline is reached after flushing with N_2. PdAu resistive sensor presents accurate measurements for each concentration, with only 0.04% H_2 maximal difference with set point (from 2.1 to 3%H_2), see Fig. 7.a. However, reaching a plateau is quite long and only happens in the last minutes of exposure. A possible reason is the high volume of the cross test chamber that may induce long filling time preventing fast signal stabilization, as it was suggested in previous work [46]. In contrast, TC commercial sensor tends to underestimate the hydrogen concentration on most of the test range. The most accurate measurement is only reached at concentration from 0.1 to 0.3% H_2, with a difference less than 0.03% H_2, while, maximal difference is obtained at 3% H_2 with 0.13% H_2 difference, see Fig. 7.a and b. Yet, as shown by the error bars on the graph, the sensor always respects the accuracy given by its data sheet, and a stable signal is reached in minute order. Sensor underestimate may originate from the low 100 sccm gas flow rate used in the test. Indeed, calibration has to be performed at 200 sccm or higher. Thus, both sensors are able to follow different dynamics of hydrogen concentration variation in N_2 anaerobic environment, either a sudden increase or a progressive fluctuation. These results are of importance, as hydrogen concentration in gas pipeline may vary overtime with either progressive fluctuation or a sudden change; thus sensors must accommodate to all operating modes. Sensors are sensitive to hydrogen concentration from 0.1 or 0.3 to 3% with 0.1% being the lower detection limit.

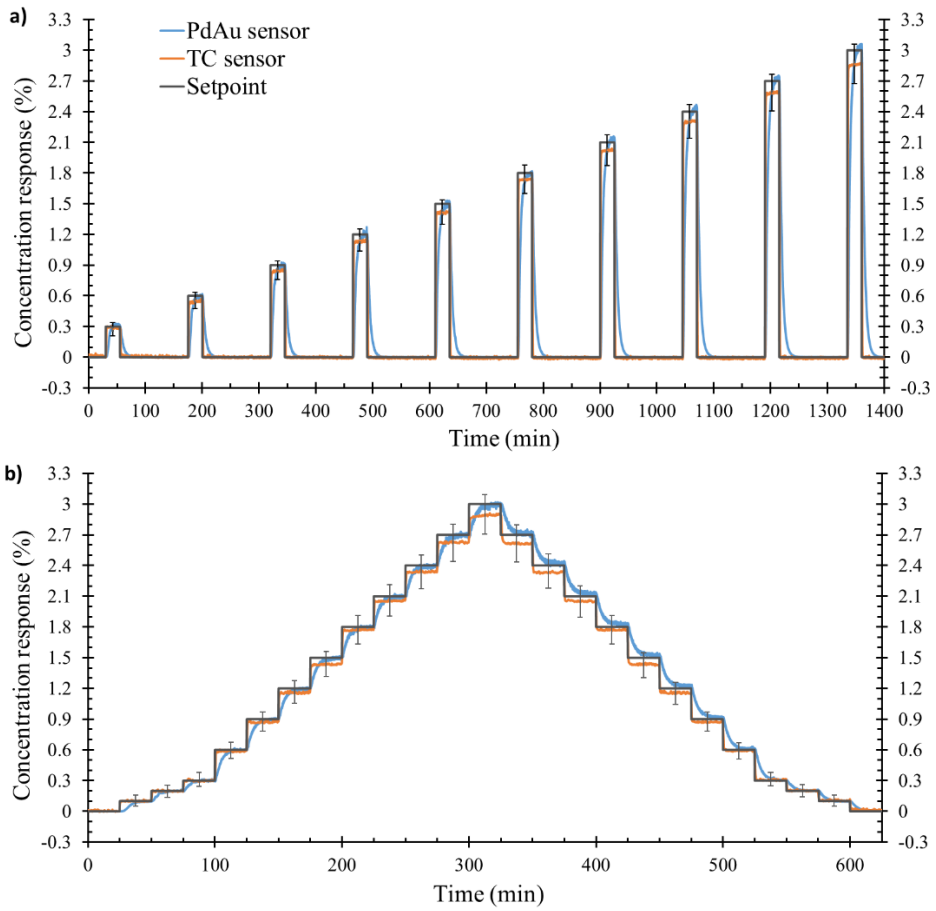

Fig. 7. Concentration response profile of PdAu sensor and commercial TC sensor for a) Pulse exposure & b) Step exposure.

4.2. Sensors hysteresis

Sensors were exposed to a continuous flow of hydrogen in N_2 following the step exposure profile in configuration 1 at a flow rate of 100 sccm.

Hysteresis values are displayed on Fig. 8. It can be seen that, for both sensors, the concentration response difference is small. For PdAu sensor, difference in C_R(%) is at most 0.028% for 2.1% H_2 and almost always positive. This implies that hydrogen measurement is slightly overestimated in decreasing phase with a maximal error of only 0.028% H_2. Hydrogen absorption hysteresis in pure Pd is large and usually reported to occur at an equilibrium pressure of 3 kPa [47] (3% H_2 at atmospheric pressure) due to the phase transition [40]. This gives rise to an uncertainty in sensor hydrogen concentration readout, which must be suppressed. Addition of gold (20-25%) allows to inhibit the phase transition, resulting in almost no hysteresis [41]. As shown in Fig. 8, addition of gold in our sensor has efficiently reduced hysteresis, making the readout uncertainty negligible. For TC sensor, there is no physical reason in its operating principle for hysteresis to be observed, and this is confirmed by Fig. 8 showing very low values fluctuating around zero. These results show that both sensors are able to follow hydrogen concentration fluctuations with a minimal error on measurement, a complete baseline recover and a lower detection limit of at least 0.1%H_2.

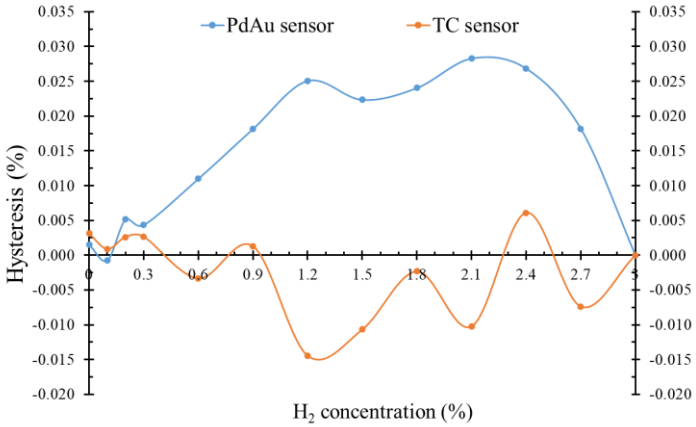

Fig. 8. Sensors hysteresis (concentration response difference on descending and rising phase) performed with step exposure profile.

4.3. Response and recovery times

The sensors response and recovery times were determined using previously described characterization parameters on the pulse exposure profile. In order to check whether the response and recovery times measured are only linked to the physico-chemical properties of the sensitive element, and not impacted by chamber filling time. The same test was repeated for different gas flows (100, 200, 300 & 400 sccm). PdAu resistive sensor was tested in configuration 1, while TC commercial sensor was first tested in configuration 1 and then in configuration 2 with cross chamber placed upstream to study filling time.

Fig. 9.a) focuses on the 3% hydrogen exposure and flushing of PdAu sensor. The sensor signal profile clearly shows that response and recovery times are influenced by gas flow. Indeed, by increasing gas flow rate, the plateau is reached faster from 9.3 min for 100 sccm to 3.4 min for 400 sccm. Similar behaviour is observed for recovery time with 10.4 min at 100 sccm to 3.3 min at 400 sccm. Further evidence is that, for a given gas flow rate, the response and recovery times are similar, regardless of the hydrogen concentration. Fig. 10.a) & .b) show a standard deviation of 0.3 min or smaller, for both response and recovery times for all gas flows (with exception of recovery time at 100 sccm), so, absorption times tend to be equivalent. In palladium based thin films, these times are normally influenced by the diffusion of atomic hydrogen into the material, which depends on the concentration of hydrogen in the atmosphere, as long as the rate of decomposition of H_2 at the palladium surface does not limit it. For these two reasons, we can conclude that the cross chamber does not allow a correct measurement of the response time of the sensors.

TC sensor results, in configuration 1, suggest that filling time is instantaneous as all response curves overlap, see Fig. 9.b). It presents an almost constant response and recovery times on all hydrogen concentration range, which is consistent with its principle, since it does not involve adsorption and diffusion [43]. Furthermore, response and recovery time value do not change with gas flow. At 100 sccm response and recovery times are about 50s with a standard deviation of 5s, similar values are obtained at 400 sccm with 45s (T90) and 40s (T10) with a standard deviation of 5s, see Fig. 10.a) & .b). However, given the poor data rate, only 1 point every 10s, previous results are an approximation of reality. Sensor concentration response tends to be slightly lower at 100 sccm for each concentration. This difference may originate from the low gas flow as mentioned earlier, yet not being specified in supplier technical data.

TC sensor was then placed in configuration 2, with cross chamber upstream, the pulse exposure profile was repeated for all 4 gas flows. The sensor signal profile at 3% H_2 presented in Fig. 9.c) shows a similar aspect to PdAu resistive sensor one, with signal stabilization reached faster with increased gas flow. Response and recovery times of both sensors are close with respectively 9.4 min (T90) and 9.7 min (T10) and standard deviation of 0.6 min and 0.4 min at 100 sccm. Response and recovery times are a little shorter at 400 sccm than PdAu sensor, with respectively 2.4 min and 2.7 min, with a standard deviation of 0.15 min and 0.30 min, see Fig. 10.a) & .b). These results confirm the filling time effect of the high volume cross chamber.

To measure accurately PdAu resistive sensor response and recovery times, a new test chamber, “boat type” [46], was developed with a volume of only 2.4 cm^3. But given actual sensor dimension, fitting was impossible, thus a part was cut off and placed in the new chamber. To confirm the fast filling time of the boat chamber, TC sensor was once again placed downstream, in configuration 2. The pulse exposure profile was performed once at 200 sccm. Unlike previous testing in cross chamber, the response and recovery times are dependent to the hydrogen concentration. Longest response and recovery times were reached at 0.3% H_2 with 3.7 and 4.5 min respectively,

shortest response and recovery times were reached at 3% H_2 with 1.3 min, see Fig. 10.c). These long measured times may be due to the density and the large film thickness (120nm), as modelling work [48] suggests that the absorption time depends mainly on the latter. This dependence was demonstrated by Wadell [32], who succeeded in reducing the response time of his 25% PdAu alloy from 5s to 1s, for exposure to 4 kPa of H_2, by decreasing both the thickness and the diameter of the nanoparticles. Thus, a sub-minute response time can be achieved with additional improvements such as a thinner film and optimised design. TC sensor presents almost identical results to configuration 1, thus confirming the instant filling of the new test chamber.

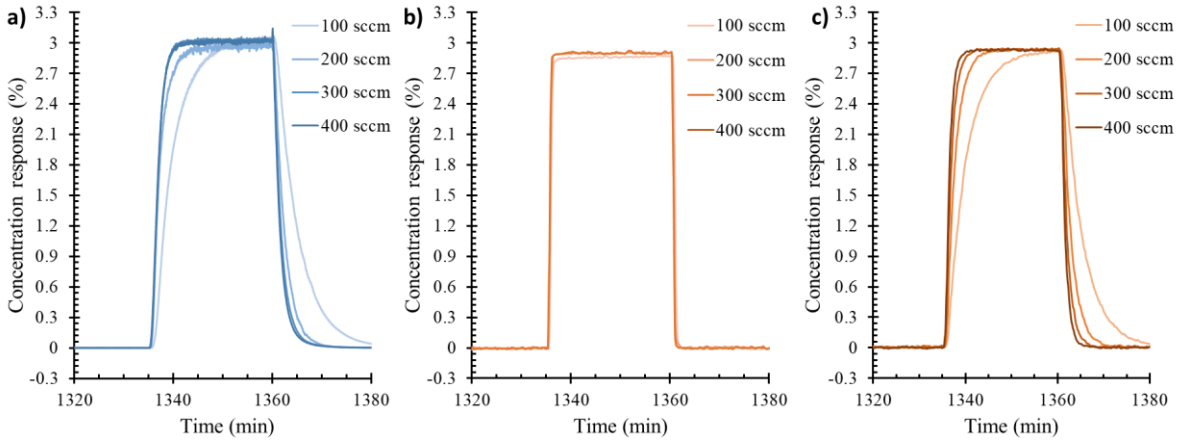

Fig. 9. Sensors pulse exposure profile for different gas flow, focus on 3%H_2 exposition; a) for PdAu sensor in the cross chamber in configuration 1, b) for TC sensor in configuration 1, c) for TC sensor in configuration 2 (after cross chamber).

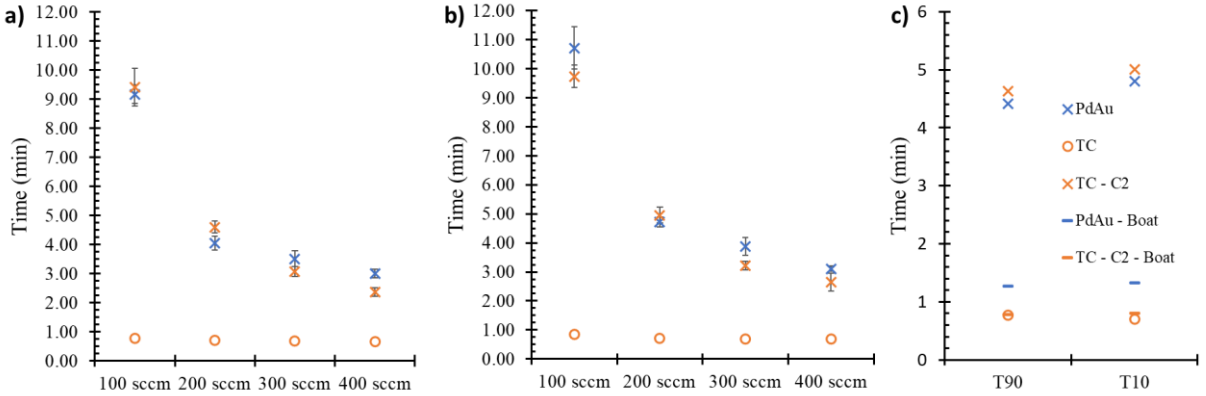

Fig. 10. Average a) response, b) recovery, time with standard deviation for PdAu and TC sensor in function of gas flow, in configuration 1 and 2. c) response and recovery time for 3% H_2 exposure at 200 sccm for all tested configurations. Cross symbol indicates that the cross chamber was used in testing, dash symbol indicates the use of boat chamber, circle is used when TC sensor operates on its own.

4.4. Selectivity to interfering gas species

For this selectivity test, the resistive and thermal conductivity sensors were placed in configuration 2. To ensure accurate measurements, gas flow was fixed at 200 sccm. As explained in part 2, sensors were exposed to hydrogen pulses at 0.9% content, in atmospheres containing interfering species. Hydrogen pulses were performed in pure N_2 for reference, in N_2 mixtures containing 20%, 40%, 70% CH_4 and in synthetic natural gas. An exposure to pure CH_4 was also performed; only X^i_0(%) result is shown as no H_2 pulse was performed. Results are presented in Fig. 11 and interfering gases exposure profile with CH_4 in Fig. 12.

Sensor response to interfering gases (X^i_0(%)):

- As expected, resistive PdAu based sensor was found to be insensitive to all interfering species, no matter the content. Without oxygen and high temperature, no hydrocarbon oxidation is possible. Thus sensor concentration response remains null and baseline constant, as shown in Fig. 11.a); X^i_0(%) factor for PdAu sensor do not appear. This is confirmed by Fig. 12, which shows that the sensor responses are only obtained for hydrogen exposures; regardless of the methane content, the baseline remains zero.
- Differently, TC sensor was found to be quite sensitive to CH_4 and other interfering gases, see Fig. 11.a). Sensor baseline gradually shift to higher responses values with methane content, as shown on Fig. 12.

The final exposure of 100% CH_4 gives a X^i_0(%) factor of about 14%. This implies that, for TC sensor, 100% CH_4 is roughly equivalent to 14% H_2 in N_2. The sensor response was found to be reversible, as initial baseline value was found back once flushing with pure N_2. Exposure to natural gas results in a sensor response similar to that obtained at 70% CH_4, but with a lower value, 9.2% versus 10.3%. This can be explained as NG contains nearly 70% CH_4 (72.06%) but also other species with lower thermal conductivity, such as CO_2. In light of these results, the TC sensor is sensitive to gas components other than hydrogen, which will lead to false hydrogen measurements. An alternative would be to recalibrate the sensor in the new carrier gas containing interfering gases. Calibration of the commercial sensor in natural gas allowed the baseline to be reset, as shown in Fig. 11.a). Hydrogen exposures with natural gas calibration will be performed and discussed below.

Sensor response to hydrogen under interfering gas (X^i_H (%)):

- Once again, PdAu based resistive sensor shows high selectivity to hydrogen. Despite being exposed to various hydrocarbons, almost no impact on sensor response to hydrogen was observed on Fig. 11.b). Variation of sensor response X^i_H(%) is as little as 1.5% at maximum, positively or negatively. This means that dissociation of H_2 molecule and H absorption into the bulk are not impacted by natural gas components and their fluctuations.
- On the contrary, for TC sensors, results on Fig. 11.b) clearly show a trend to response attenuation by increasing methane content. A 7.7% response reduction is observed for 70% CH_4. In natural gas, hydrogen response is even lower with 8.7% reduction compared to operation in pure N_2. Recalibration in natural gas does not improve the selectivity of the sensor, on the contrary, with a decrease of almost 42% in the sensor response. Thus, methane and natural gas have an interfering effect on the hydrogen response of the TC sensor.

These results confirm the observations from other works [30], [31], [49], and only PdAu sensor is able to measure accurate hydrogen concentrations in a mixture of N_2/CH_4 and in natural gas, without interfering effect. In addition, the resistive sensor is only sensitive to hydrogen element among all the components of the synthetic natural gas. However, as mentioned by Darmadi et al [50], PdAu materials are sensitive to CO poisoning, which is a pollutant that may be present in NG pipelines. It was suggested [40], [50], that protective polymer coatings or Cu alloying, may be sufficient to protect completely from this effect, thus allowing their use as hydrogen sensor in natural gas medium.

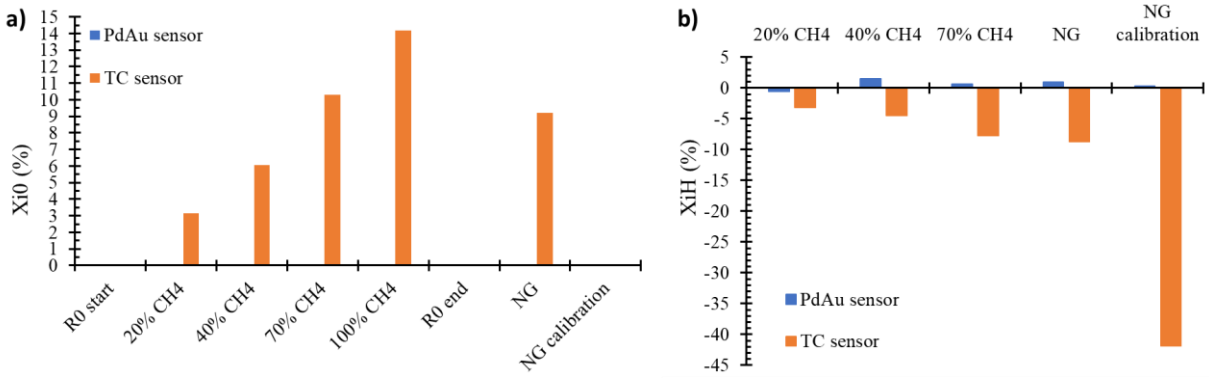

Fig. 11. a) baseline variation (X^i_0 (%)), b) sensor response percentage variation (X^i_H (%)), of PdAu and TC sensors for different interfering gas and content.

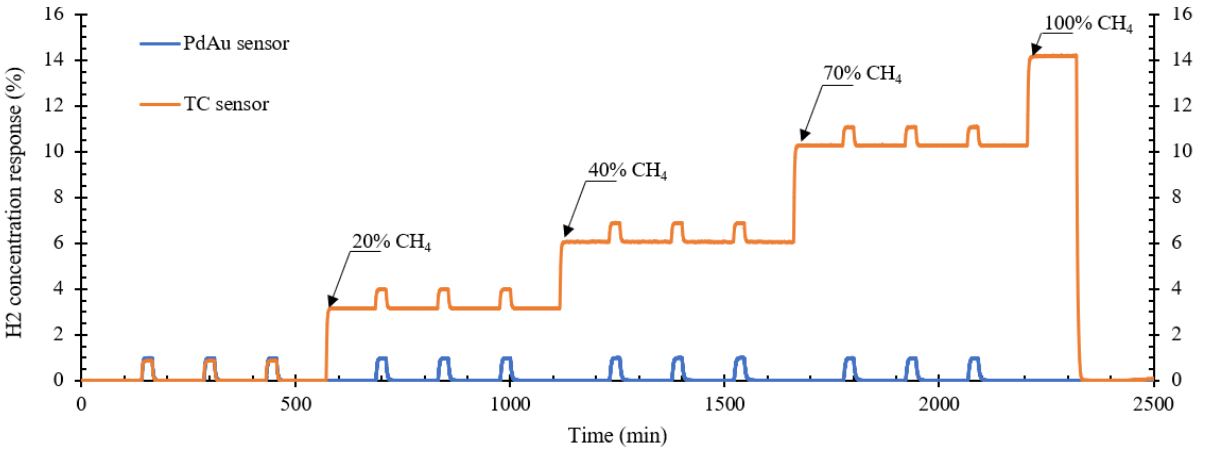

Fig. 12. Interfering gas exposure profile of PdAu and TC sensor at 200 sccm. H_2 exposure starts in pure N_2, then CH_4 is mixed with N_2 at 20%, 40%, 70% content. Finally pure CH_4 is injected and then flushed with pure N_2.

5. Conclusion

In this paper, two hydrogen sensors, one based on thermal conductivity (TC) measurement, and the other using a resistive thin film of Pd alloy, were tested in anaerobic environments. The results of our study, summarised in Table 2, show that both sensors are able to detect H_2 in anaerobic environments, in the concentration range of our test (0.1% to 3% H_2) with different dynamics of variation of the hydrogen concentration (0.3% increase per step or per pulse). Measurements are repeatable over the entire exposure range. Flow rate should be 200 sccm or higher for TC gas sensor, otherwise it may underestimate hydrogen concentration and increase measurement time. Hysteresis of the two sensors is very low, thus sensors can follow small concentration fluctuations accurately. PdAu measurement time is 80s at 3% H_2 while it is 50s at any hydrogen concentration for TC gas sensor. However, present work highlights that TC gas sensors are sensitive to the surrounding atmosphere constituents and their thermal conductivity. A change in gas composition, other than H_2 or N_2, will cause a baseline drift which will result in false measurements. Therefore, TC gas sensor is not suitable for H_2 measurement in a natural gas medium. On the contrary, the PdAu sensor is only sensitive to H_2, when exposed to natural gas atmosphere composed of various hydrocarbons, CO_2 and N_2. In conclusion, resistive Pd alloy based sensors are very efficient devices to measure and monitor the evolution of H_2 concentration in natural gas, with variable gas quality, and are thus promising for P2G technology. In the light of these results, PdAu resistive sensor design will be reworked and material optimized to reach sub minute response and recovery times.

Sensors	Thermal conductivity (TC)	Palladium gold resistive (PdAu)
Lower test concentration (% H_2)	0.10	
Detection range (% H_2)	[0.1; 3] for 0.3% step or pulse variation	
Hysteresis (%)	< 0.014	< 0.028
Response and recovery time (s)	50 (at any % H_2)	80 (at 3% H_2)
Gas flow rate (sccm)	>200	Any
Selectivity to H_2 in CH_4 and NG	Sensitive to CH_4 and NG	H_2 only

Table 2. Sensor performance summary for hydrogen detection in anaerobic and natural gas environment.

6. Acknowledgements

This work was supported by Région Sud of France and CMR Group.

The authors thank Soilihi Moindjie, Jean-Jacques Furter for their technical support and Khaoula EL Ouazzani for performing XRD.

References

[1] A. Demirbas, 'Future hydrogen economy and policy', *Energy Sources, Part B: Economics, Planning, and Policy*, vol. 12, no. 2, pp. 172–181, Feb. 2017, doi: 10.1080/15567249.2014.950394.

[2] C. Acar and I. Dincer, 'Review and evaluation of hydrogen production options for better environment', *Journal of Cleaner Production*, vol. 218, pp. 835–849, May 2019, doi: 10.1016/j.jclepro.2019.02.046.

[3] Z. Abdin, A. Zafaranloo, A. Rafiee, W. Mérida, W. Lipiński, and K. R. Khalilpour, 'Hydrogen as an energy vector', *Renewable and Sustainable Energy Reviews*, vol. 120, p. 109620, Mar. 2020, doi: 10.1016/j.rser.2019.109620.

[4] G. Kakoulaki, I. Kougias, N. Taylor, F. Dolci, J. Moya, and A. Jäger-Waldau, 'Green hydrogen in Europe – A regional assessment: Substituting existing production with electrolysis powered by renewables', *Energy Conversion and Management*, vol. 228, p. 113649, Jan. 2021, doi: 10.1016/j.enconman.2020.113649.

[5] R. Fleming, 'Clean or renewable – hydrogen and power-to-gas in EU energy law', *Journal of Energy & Natural Resources Law*, vol. 39, no. 1, pp. 43–63, Jan. 2021, doi: 10.1080/02646811.2020.1795382.

[6] D. Haeseldonckx and W. D'haeseleer, 'The use of the natural-gas pipeline infrastructure for hydrogen transport in a changing market structure', *International Journal of Hydrogen Energy*, vol. 32, no. 10, pp. 1381–1386, Jul. 2007, doi: 10.1016/j.ijhydene.2006.10.018.

[7] A. Maroufmashat and M. Fowler, 'Transition of Future Energy System Infrastructure; through Power-to-Gas Pathways', *Energies*, vol. 10, no. 8, p. 1089, Jul. 2017, doi: 10.3390/en10081089.

[8] M. Kong, S. Feng, Q. Xia, C. Chen, Z. Pan, and Z. Gao, 'Investigation of Mixing Behavior of Hydrogen Blended to Natural Gas in Gas Network', *Sustainability*, vol. 13, no. 8, p. 4255, Apr. 2021, doi: 10.3390/su13084255.

[9] G. Guandalini, S. Campanari, and M. C. Romano, 'Power-to-gas plants and gas turbines for improved wind energy dispatchability: Energy and economic assessment', *Applied Energy*, vol. 147, pp. 117–130, Jun. 2015, doi: 10.1016/j.apenergy.2015.02.055.

[10] S. Ouchikh, M. S. Lounici, L. Tarabet, K. Loubar, and M. Tazerout, 'Effect of natural gas enrichment with hydrogen on combustion characteristics of a dual fuel diesel engine', *International Journal of Hydrogen Energy*, vol. 44, no. 26, pp. 13974–13987, May 2019, doi: 10.1016/j.ijhydene.2019.03.179.

[11] Y. Park, M. Choi, D. Kim, J. Lee, and G. Choi, 'Performance analysis of large-scale industrial gas turbine considering stable combustor operation using novel blended fuel', *Energy*, vol. 236, p. 121408, Dec. 2021, doi: 10.1016/j.energy.2021.121408.

[12] S. Benaissa, B. Adouane, S. M. Ali, S. S. Rashwan, and Z. Aouachria, 'Investigation on combustion characteristics and emissions of biogas/hydrogen blends in gas turbine combustors', *Thermal Science and Engineering Progress*, vol. 27, p. 101178, Jan. 2022, doi: 10.1016/j.tsep.2021.101178.

[13] GRTgaz, 'Jupiter 1000 - Power-to-Gas - Project', *Jupiter1000*. https://www.jupiter1000.eu/projet (accessed Sep. 16, 2022).

[14] K. Birkitt, M. Loo-Morrey, C. Sanchez, and L. O'Sullivan, 'Materials aspects associated with the addition of up to 20 mol% hydrogen into an existing natural gas distribution network', *International Journal of Hydrogen Energy*, vol. 46, no. 23, pp. 12290–12299, Mar. 2021, doi: 10.1016/j.ijhydene.2020.09.061.

[15] T. T. Nguyen, J. Park, W. S. Kim, S. H. Nahm, and U. B. Beak, 'Effect of low partial hydrogen in a mixture with methane on the mechanical properties of X70 pipeline steel', *International Journal of Hydrogen Energy*, vol. 45, no. 3, pp. 2368–2381, Jan. 2020, doi: 10.1016/j.ijhydene.2019.11.013.

[16] K. Altfeld and D. Pinchbeck, 'Admissible hydrogen concentrations in natural gas systems', *Gas for Energy*, p. 12, 2013.

[17] H. K. Kayadelen, 'Effect of natural gas components on its flame temperature, equilibrium combustion products and thermodynamic properties', *Journal of Natural Gas Science and Engineering*, vol. 45, pp. 456–473, Sep. 2017, doi: 10.1016/j.jngse.2017.05.023.
[18] D. J. Abbott, J. P. Bowers, and S. R. James, 'The impact of natural gas composition variations on the operation of gas turbines for power generation', presented at the Proceedings of the 6th International Conference on the Future of Gas Turbine Technology, Brussels, Belgium, 2012, pp. 17–18.
[19] Y. S. Najjar, 'Hydrogen Leakage Sensing and Control: (Review)', *BJSTR*, vol. 21, no. 5, Oct. 2019, doi: 10.26717/BJSTR.2019.21.003670.
[20] M. Chaczykowski and P. Zarodkiewicz, 'Simulation of natural gas quality distribution for pipeline systems', *Energy*, vol. 134, pp. 681–698, Sep. 2017, doi: 10.1016/j.energy.2017.06.020.
[21] L. Boon-Brett *et al.*, 'Identifying performance gaps in hydrogen safety sensor technology for automotive and stationary applications', *International Journal of Hydrogen Energy*, vol. 35, no. 1, pp. 373–384, Jan. 2010, doi: 10.1016/j.ijhydene.2009.10.064.
[22] L. Boon-Brett, J. Bousek, and P. Moretto, 'Reliability of commercially available hydrogen sensors for detection of hydrogen at critical concentrations: Part II – selected sensor test results', *International Journal of Hydrogen Energy*, vol. 34, no. 1, pp. 562–571, Jan. 2009, doi: 10.1016/j.ijhydene.2008.10.033.
[23] A. S. Ruhl and A. Kranzmann, 'Investigation of corrosive effects of sulphur dioxide, oxygen and water vapour on pipeline steels', *International Journal of Greenhouse Gas Control*, vol. 13, pp. 9–16, Mar. 2013, doi: 10.1016/j.ijggc.2012.12.007.
[24] D. V. Del Orbe *et al.*, 'Low-power thermocatalytic hydrogen sensor based on electrodeposited cauliflower-like nanostructured Pt black', *Sensors and Actuators B: Chemical*, vol. 329, p. 129129, Feb. 2021, doi: 10.1016/j.snb.2020.129129.
[25] S.-W. Jung, E. K. Lee, J. H. Kim, and S.-Y. Lee, 'High-concentration Nafion-based hydrogen sensor for fuel-cell electric vehicles', *Solid State Ionics*, vol. 344, p. 115134, Jan. 2020, doi: 10.1016/j.ssi.2019.115134.
[26] A. Miyamoto *et al.*, 'Solid Electrolyte Gas Sensor Based on a Proton-Conducting Graphene Oxide Membrane', *ACS Omega*, vol. 2, no. 6, pp. 2994–3001, Jun. 2017, doi: 10.1021/acsomega.7b00239.
[27] Y. Luo, C. Zhang, B. Zheng, X. Geng, and M. Debliquy, 'Hydrogen sensors based on noble metal doped metal-oxide semiconductor: A review', *International Journal of Hydrogen Energy*, vol. 42, no. 31, pp. 20386–20397, Aug. 2017, doi: 10.1016/j.ijhydene.2017.06.066.
[28] W.-T. Koo *et al.*, 'Chemiresistive Hydrogen Sensors: Fundamentals, Recent Advances, and Challenges', *ACS Nano*, vol. 14, no. 11, pp. 14284–14322, Nov. 2020, doi: 10.1021/acsnano.0c05307.
[29] T. Hübert, L. Boon-Brett, G. Black, and U. Banach, 'Hydrogen sensors – A review', *Sensors and Actuators B: Chemical*, vol. 157, no. 2, pp. 329–352, Oct. 2011, doi: 10.1016/j.snb.2011.04.070.
[30] W. J. Buttner *et al.*, 'Inter-laboratory assessment of hydrogen safety sensors performance under anaerobic conditions', *International Journal of Hydrogen Energy*, vol. 37, no. 22, pp. 17540–17548, Nov. 2012, doi: 10.1016/j.ijhydene.2012.03.165.
[31] R. J. Westerwaal *et al.*, 'Fiber optic hydrogen sensor for a continuously monitoring of the partial hydrogen pressure in the natural gas grid', *Sensors and Actuators B: Chemical*, vol. 199, pp. 127–132, Aug. 2014, doi: 10.1016/j.snb.2014.03.048.
[32] C. Wadell, F. A. A. Nugroho, E. Lidström, B. Iandolo, J. B. Wagner, and C. Langhammer, 'Hysteresis-Free Nanoplasmonic Pd–Au Alloy Hydrogen Sensors', *Nano Lett.*, vol. 15, no. 5, pp. 3563–3570, May 2015, doi: 10.1021/acs.nanolett.5b01053.
[33] F. A. A. Nugroho, I. Darmadi, V. P. Zhdanov, and C. Langhammer, 'Universal Scaling and Design Rules of Hydrogen-Induced Optical Properties in Pd and Pd-Alloy Nanoparticles', *ACS Nano*, vol. 12, no. 10, pp. 9903–9912, Oct. 2018, doi: 10.1021/acsnano.8b02835.

[34] C. Occelli, T. Fiorido, C. Perrin-Pellegrino, and J.-L. Seguin, 'PdAu Based Resistive Hydrogen Sensor in Anaerobic Environment', in *SENSORCOMM 2021*, Athen, Greece, Nov. 2021. Accessed: Jul. 25, 2022. [Online]. Available: https://hal-amu.archives-ouvertes.fr/hal-03428722
[35] K. Yu, X. Tian, X. Wang, F. Yang, T. Qi, and J. Zuo, 'Enhanced accuracy of palladium-nickel alloy based hydrogen sensor by in situ temperature compensation', *Sensors and Actuators B: Chemical*, vol. 299, p. 126989, Nov. 2019, doi: 10.1016/j.snb.2019.126989.
[36] P. Tripodi *et al.*, 'The effect of hydrogenation/dehydrogenation cycles on palladium physical properties', *Physics Letters A*, vol. 373, no. 35, pp. 3101–3108, Aug. 2009, doi: 10.1016/j.physleta.2009.06.057.
[37] E. Lee, J. M. Lee, J. H. Koo, W. Lee, and T. Lee, 'Hysteresis behavior of electrical resistance in Pd thin films during the process of absorption and desorption of hydrogen gas', *International Journal of Hydrogen Energy*, vol. 35, no. 13, pp. 6984–6991, Jul. 2010, doi: 10.1016/j.ijhydene.2010.04.051.
[38] S. Dekura *et al.*, 'The Electronic State of Hydrogen in the α Phase of the Hydrogen-Storage Material PdH(D)x: Does a Chemical Bond Between Palladium and Hydrogen Exist?', *Angewandte Chemie International Edition*, vol. 57, no. 31, pp. 9823–9827, 2018, doi: 10.1002/anie.201805753.
[39] Y. Sakamoto, F. L. Chen, M. Ura, and T. B. Flanagan, 'Thermodynamic Properties for Solution of Hydrogen in Palladium-Based Binary Alloys', *Berichte der Bunsengesellschaft für physikalische Chemie*, vol. 99, no. 6, pp. 807–820, Jun. 1995, doi: 10.1002/bbpc.19950990605.
[40] I. Darmadi, F. A. A. Nugroho, and C. Langhammer, 'High-Performance Nanostructured Palladium-Based Hydrogen Sensors—Current Limitations and Strategies for Their Mitigation', *ACS Sens.*, p. acssensors.0c02019, Nov. 2020, doi: 10.1021/acssensors.0c02019.
[41] S. Luo, D. Wang, and T. B. Flanagan, 'Thermodynamics of Hydrogen in fcc Pd−Au Alloys', *J. Phys. Chem. B*, vol. 114, no. 18, pp. 6117–6125, May 2010, doi: 10.1021/jp100858r.
[42] Z. Zhao and M. A. Carpenter, 'Annealing enhanced hydrogen absorption in nanocrystalline Pd⁄Au sensing films', *Journal of Applied Physics*, vol. 97, no. 12, p. 124301, Jun. 2005, doi: eff.
[43] D. Berndt *et al.*, 'MEMS-based thermal conductivity sensor for hydrogen gas detection in automotive applications', *Sensors and Actuators A: Physical*, vol. 305, p. 111670, Apr. 2020, doi: 10.1016/j.sna.2019.111670.
[44] T. Harumoto, H. Fujiki, J. Shi, and Y. Nakamura, 'Extremely simple structure hydrogen gas sensor based on single metallic thin-wire under sweep heating', *International Journal of Hydrogen Energy*, vol. 47, no. 80, pp. 34291–34298, Sep. 2022, doi: 10.1016/j.ijhydene.2022.08.001.
[45] BlueSens, 'BlueVary Brochure'. [Online]. Available: https://www.bluesens.com/fileadmin/user_upload/downloads-products/BlueVary/BlueVary%20Brochure%20EN.pdf
[46] F.-E. Annanouch *et al.*, 'Hydrodynamic evaluation of gas testing chamber: Simulation, experiment', *Sensors and Actuators B: Chemical*, vol. 290, pp. 598–606, Jul. 2019, doi: 10.1016/j.snb.2019.04.023.
[47] M. Fisser, R. A. Badcock, P. D. Teal, and A. Hunze, 'Optimizing the sensitivity of palladium based hydrogen sensors', *Sensors and Actuators B: Chemical*, vol. 259, pp. 10–19, Apr. 2018, doi: 10.1016/j.snb.2017.11.180.
[48] Y. Liu, Y. Li, P. Huang, H. Song, and G. Zhang, 'Modeling of hydrogen atom diffusion and response behavior of hydrogen sensors in Pd–Y alloy nanofilm', *Scientific Reports*, vol. 6, no. 1, pp. 1–9, Nov. 2016, doi: 10.1038/srep37043.
[49] V. Palmisano *et al.*, 'Evaluation of selectivity of commercial hydrogen sensors', *International Journal of Hydrogen Energy*, vol. 39, no. 35, pp. 20491–20496, Dec. 2014, doi: 10.1016/j.ijhydene.2014.03.251.
[50] I. Darmadi, S. Z. Khairunnisa, D. Tomeček, and C. Langhammer, 'Optimization of the Composition of PdAuCu Ternary Alloy Nanoparticles for Plasmonic Hydrogen Sensing', *ACS Appl. Nano Mater.*, p. acsanm.1c01242, Aug. 2021, doi: 10.1021/acsanm.1c01242.